UDC 629.7.014-519-226.2:534.2:519.6 **doi: 10.32620/aktt.2024.2.02**

Petro LUKIANOV, Oleg DUSHEBA

National Technical University of Ukraine
"Igor Sikorsky Kyiv Polytechnic Institute", Kyiv, Ukraine

NUMERICAL STUDY OF THE INFLUENCE OF QUADROTOR BLADE PARAMETERS ON AERODYNAMIC NOISE GENERATION

The aim of this *paper is to study the effect of variation of the parameters of a small-sized quadrotor blade on the level of aerodynamic noise and its frequency spectrum. There is a certain discrepancy between the calculated and experimental data available today. The reason for this is that the study of quadrotor rotor noise is carried out using various theoretical models that do not consider certain factors of sound generation or additional artificial sound sources, which result in an overestimated noise level. Therefore, there is a need for an accurate model, the calculation of which more closely matches the experimental data. In the paper below, an aerodynamic noise model is proposed to study the noise of a quadrocopter blade, which considers the non-stationarity and three-dimensionality of the sound generation and propagation process.* ***The research methods are based on*** *the numerical calculation of the characteristics of the near and far sound fields in the potential approximation: pressure coefficient, sound pressure level, and spectrum of the generated sound. The main parameters that were varied during numerical calculations were the rotor speed of the quadrotor, angle of attack, torsion angle, and blade position in the plane of rotation. The NASA parabolic profile was used as the test profile.* ***Results and conclusions****. The results of numerical calculations in the near field revealed three areas of sound generation above the blade surface. The first region, which is more unstable, is caused by blade torsion. The other two sound generation areas are smoothly distributed along the blade's swing, and the pressure change level in each of them doubles. The level of generated aerodynamic noise is largely dependent on the blade speed and the distance from the blade at which the noise is calculated. The angle of attack and blade pitch have a smaller effect on the generated noise level, and in the far field, they have almost no effect on the maximum noise level. The dependence of noise on the distance to the blade, as well as the blade parameters, which were chosen similar to those studied by other authors, showed a fairly good agreement with the calculations of these authors and with experimental studies. Because of aerodynamic calculations and noise generation around the quadrotor blade using ANSYS software, it was found that sound vibrations occur during the flow around the blade tip, with a level of 120 dB in the immediate vicinity of the blade surface. Calculations using a 3D model of the propeller confirmed that the volume reached 80 dB at the nearest reference point, which closely matches the data from the calculation based on the potential model and the experimental data.*

Keywords*: aerodynamic noise; numerical methods; quadrocopter.*

Introduction

The designs of modern vertical take-off and landing (VTOL) aircraft are constantly being improved, taking on new forms. This modernisation also applies to the rotor blades of helicopters, air taxis and quadcopters. The rotation of the rotor blades generates aerodynamic noise. Due to the emergence of new VTOL designs and new rotor blade shapes, the problem of reducing this type of noise remains relevant, as each new blade must be tested for noise. According to the requirements of international organisations for regulating the level of noise in the area [1], the propellers must meet the volume standards and be low-noise. And these standards are being tightened from year to year, stimulating further search for low-noise propeller blade shapes.

Attempts to reduce the noise of the blade of aerodynamic origin face certain contradictions: changing the shape of the propeller blade to improve aerodynamic or dynamic characteristics can lead to an increase in noise of aerodynamic origin, and vice versa. Thus, the rotor design problem requires a comprehensive solution that includes both the calculation of aerodynamic and acoustic characteristics. Existing publications in the field of quadrotor improvement are mostly devoted to improving the aerodynamic layout and calculation of rotors, studying the possibilities of using modern electric motors of sufficient power with a relatively small weight, and finding suitable power sources for them. The problem of studying the noise of aerodynamic quadrocopters has also recently begun to receive more and more attention. The reason is the sharp increase in the number of drones used in populated areas

ISSN 1814-4225 (print)
ISSN 2663-2012 (online)

over the past decade, which has led to noise pollution. Here we will analyse the available publications related to numerical modelling and experimental study of quadrotor rotor noise.

1. Analysis of existing studies of quadrotor rotor noise

In [2], an analytical simplified method (low-fidelity) is proposed for modelling the noise of the interaction between the vortex wake and the blade (BWI- blade wake interaction). This method takes into account the interaction of the blade and the vortex shroud. The results of the numerical calculation for R=2.25m, c=0.23m show that the maximum sound pressure level (SPL) corresponds to 82dB at a frequency of 500Hz. In addition, the effect of noise distribution in different areas of the space around the blade, as well as the effect of the angle of attack on the generated noise level, was studied.

The study of the rotor noise of a helicopter-type air taxi with a quiet rotor is devoted to [3]. It investigates tone, broadband noise, load noise, and thickness noise. The aerodynamic calculation was performed on the basis of the Froude blade element theory [4]. The acoustic calculation was based on the Farassat formula [5]. The calculated data obtained in different positions relative to the rotor blades showed that broadband noise dominates for low blade end velocities and for a larger number of blades. For high blade end velocities and a small number of blades, the level of tonal noise is comparable in magnitude to that of broadband noise.

Paper [6] considers the characteristics of quadrotor propellers of small radii, R = 0.15 cm, operating at reduced Reynolds numbers, up to 10^5. The numerical calculation of the distribution of the generated noise on the surface of the propeller blade showed that the highest noise level (85 dB) is generated at the end of the blade, at its trailing edge. The issue of studying the efficiency of using various modifications of vertical take-off vehicles as air taxis is addressed in [7]. It conducts a comparative analysis of VTOL noise, which indicates that a quadrotor-type air taxi has a noise level of about 85-87 dB. Paper [8] compares experimental measurements with a numerical calculation of the noise of a small rotor. A distinctive feature of this type of rotor compared to helicopter rotors is the different value of the *advance ratio* (the ratio of horizontal flight speed to the speed at the blade end) at relatively low flight speeds of the quadrotor (V=12.9 m/s). The aerodynamic calculation was carried out using various approaches: blade element theory, potential flow methods, Prandl's lift line theory, and the Navier-Stokes equation. In particular, it is noted that simplified theories (e.g., the blade element theory) provide a satisfactory match for low speeds and small blade angles in the rotor blade tip. In other cases, it is necessary to use more accurate flow models that take into account 3d effects. The calculations showed that for different values of the blade installation angles at the rotor end, the noise level varied in the range from 74dB <L< 86dB. In addition, the data on the effect of shielding on the generated noise level are interesting. For the angle at the rotor end, the noise level reaches 102dB

In a number of studies, a comparative analysis of numerical calculation data with experimental data showed that experimental and calculated noise levels differ significantly. For example, paper [9] presents data on the aerodynamic and acoustic characteristics of a small multirotor for various flight conditions. It should be noted that the maximums on the sound pressure level graphs significantly exceed the sound pressure level values obtained in the experiment. Thus, the calculation data in different positions reaches 110dB, while the experimental values are in the region of 80-85dB. This significant difference is not explained in any way. However, the reason for this may be the inaccuracy of the aerodynamic sound generation model, which takes into account "fictitious" sound sources that do not exist in reality [10]. The second factor in the difference in noise level values may be the different distance where the noise was measured.

Recently, a number of studies have been devoted to studying the compliance of the generated noise level of serial samples of quadrocopters with current regulatory standards. For example, in [11], the authors present noise measurements of DJI Mavic 2 Pr and DJI Inspire-2 quadcopters on the ground to verify compliance with the current regulatory agreement [12] on noise. Both quadcopters meet the permissible noise standards: the noise recorded by the equipment did not exceed 72 dB. Moreover, the Mavic 2 Pr is less noisy than the DJI Inspire 2.

The main theoretical issues of interest are the factors that cause the noise of quadrotor rotors, as well as the parameters that determine its level. Paper [13] classified the noise of the interaction between the blade and the vortex wake (BWI) of a quadrotor for the hovering flight mode. Its significance is shown, as well as the fact that the formation of vortex structures does not depend on the rotor thrust, but on the rotor thrust coefficient. An experimental analysis of small quadrocopters with the NACA-16 profile, whose radius is R = 0.3 m, is given in [14]. Noise measurements with microphones for different blade angles indicate that a conventional blade can generate noise at low frequencies up to 119dB. Numerical calculations give even higher noise levels - up to 120dB. Paper [15] presents an analysis of the main characteristics of small

UAVs that affect noise reduction: the number of propellers, the number of blades, the propeller radius, and the rotation speed. The paper presents a comprehensive calculation of UAV parameters for the purpose of their optimisation and noise reduction. The noise level and blade parameters corresponded to [12]. To analyse the impact of noise on the environment and measure its level, the HolyStone HS720 UAV was studied [16]. The total calculated noise level was about 86.8dB, which exceeds the permissible noise level of 85dB according to the existing ISO 3744 limits.

Paper [17] studied the dominance of certain types of noise in different flight modes of a quadrotor with propellers R = 15.2 cm, R = 8.3 cm, and a rotation frequency of Ω=4083rpm. The load noise was calculated using the Gutin formula [18]. The paper notes that the noise of a stationary force impact on the blade manifests itself mainly at low frequencies. The noise from the unsteady load, which was calculated using simplified formulas, prevails near the vertical axis of rotor rotation and dominates for the case of oblique flow blowing of the quadrotor blades. Spectral Fourier analysis showed that the pressure level in individual harmonics is 112-115 dB. In [19], an approach is used to calculate the characteristics of the flow field obtained from solving the averaged unsteady Navier-Stokes equation. The calculated flow field data were used to study the sources of noise from stationary and unsteady loading on the blade. The blade radius was R=0,17cm, the rotation speed was 5000 rpm, and the Mach number was M=0.264. The research results showed that the noise of blade-vortex interaction is significantly manifested in the 3rd and 6th harmonics of the rotation noise generated by unsteady loading on the blade.

A comprehensive theoretical study for the model-DJI 9450 propeller, with a rotor diameter of D=23.9 cm, was presented in [20]. Experimental and computational noise analysis was performed. The aerodynamic calculations have been carried out using the free wake vortex lattice method. The acoustic calculation is based on the Ffowcs Williams-Hawkings (FW-H) equations. A new approach, called the RPM fluctuation correction method, was developed to take into account the effects of frequency modulation by correcting the signals provided by classical methods for predicting the noise of helicopters. The concepts of the fluctuation depth and the fluctuation period are introduced, which take into account the variation of physical parameters during one rotation of the propeller. Using this approach, it is possible to adjust the lift and thrust coefficient within 5% to 15%. The maximum sound pressure level obtained as a result of the calculation is close to the experimental values and is about L=72dB-75dB. At the same time, the experimental noise value is slightly higher than the calculated values.

One of the directions of searching for silent blade shapes is the natural shapes of bird wings. For example, [21] emphasises that owls are noiseless night hunters. They rely on acoustic signals to locate prey, so the noise from their own wings should be minimal, which is indeed the case.

In [22], the acoustic characteristics of the DJI Phantom II quadcopter were studied for different blade shapes, as well as for different materials used to make the blades. Paper [23] presents the basic theoretical models and numerical methods for solving aeroacoustic problems for drones, implemented on the basis of ANSYS models. The calculated noise level does not exceed 82 dB, which is quite close to the available experimental data for existing drones, as discussed above. Works [24], [25] present an experimental study of various types of drone noise, including engine noise. Experimental studies of small quadcopter noise were performed. In particular, [24] established a relationship between the noise level and the distance to the quadrotor: noise measurements were carried out at distances of l=5m, 10m, 15m, and 20m. It was found that with a doubling of the distance, the noise level decreases by 6dB. The direction of maximum noise corresponds to the horizon. The highest noise level recorded in the experiment is close to 78dB. Paper [26] presents an aerodynamic calculation using the k-ε model, and the calculation of aeroacoustic noise was performed using the Fawkes-Williams-Hawkins formula. The study found that the noise from UAS increases with increasing speed, propeller speed and pitch angle.

The above analysis shows that there is no single approach (model) for a small quadrotor that allows for an accurate description of the sound of aerodynamic origin. Previous studies by the author of this paper on helicopter rotor noise and air taxis [27], [28] indicate that changes in helicopter blade parameters significantly affect noise generation, and rotor rotation noise can be described quite accurately within the model [10]. For quadrotor with small blades, little attention has been paid to this issue: the mutual dependence of rotor blade parameters on noise reduction has not been sufficiently investigated. In this regard, the authors of this paper studied the effect of changing the blade geometry along the blade span, with simultaneous variation of the angle of attack and torsion of the blade, and the rotor speed on the nature and level of generated quadrotor noise. The research data are presented below.

Objective: To study the effect of changing the parameters of small quadcopter blades on the level and nature of aerodynamic noise.

ISSN 1814-4225 (print)
АВІАЦІЙНО-КОСМІЧНА ТЕХНІКА І ТЕХНОЛОГІЯ, 2024, № 2(194) ISSN 2663-2012 (online)

2. Problem setting

Consider a quadcopter blade (Fig.1). Let's introduce the rectilinear Cartesian coordinate system Oxyz.

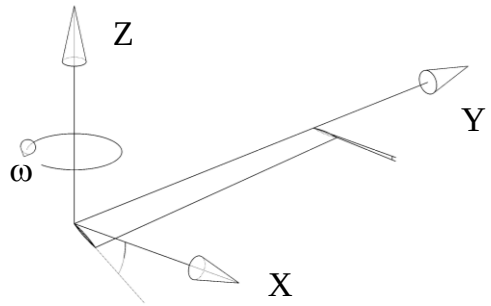

Fig.1 Rotation of the quadcopter blade

We will assume that the blade of the quadrotor is a rigid thin wing that does not deform. The sound of aerodynamic origin is generated by the interaction of this blade with the flow and represents small flow disturbances that occur in the flow layers close to the blade. However, it should not be confused with boundary layer pulsations. The sound is not generated in the boundary layer, but behind it. The equation describing the sound generation process in the three-dimensional unsteady case was previously derived in [10]. It is a second-order nonlinear partial differential equation for the potential of small flow perturbations ϕ':

$$\nabla^2\phi' - \frac{1}{a_\infty^2}\phi'_{tt} = M_1^2\{(1+(1+\gamma)\phi'_x)\phi'_{xx} + \frac{2}{U}\phi'_{xt}\}, \quad (1)$$

where x,y,z is the Cartesian coordinate system; $a_\infty, U_\infty = U$ are the sound propagation speed and the flow velocity running into the blade, respectively.
If the equation of the blade surface is given in an implicit form $F(x,y,z)=0$, then the condition of non-flow through the surface can be set:

$$F_t + \bar{v}\nabla F = 0. \quad (2)$$

Note that condition (2) is valid for the velocity in general, so it is automatically fulfilled for small sound perturbations of the velocity potential ϕ'. At the initial moment of time when the flow hits the blade, the initial perturbations are: $\phi'_{|t=0} = 0, \phi'_{t|t=0} = 0$.

3. Method of solving the problem

Equation (1) is a second-order nonlinear partial differential equation. In the part of the space region around the blade where the flow is unstable and generates sound, not every numerical scheme is able to solve the boundary value problem for equation (1). It is known that the numerical scheme [29, 30] allows us to determine the behaviour of equation (1) in different parts of the flow field and has a different finite-difference representation in each of the parts. The scheme [31], the so-called scheme of alternating directions, also allows solving equation (1) numerically. However, these schemes are presented only for a two-dimensional unsteady flow field. The numerical-analytical method developed earlier by the author [32, 33] was successfully used to solve a number of problems of noise generation by a helicopter rotor. In this paper, this method is used to study the sound generation by a small-sized quadrotor blade.

For a stable numerical solution of the boundary value problem (1) - (2), it is necessary to introduce dimensionless coordinates:

$$\xi = \frac{x}{c}, \eta = \lambda y, \zeta = \frac{z}{R}, \tau = kt, \quad (3)$$

where c is the length of the blade chord, R is its radius, and k is a dimensionless time parameter that determines the time for the flow to pass across the blade cross-section. In the dimensionless form, equation (1) will take the form:

$$\left(\frac{kc}{U}\right)^2 f_{\tau\tau} + \left[1 - \frac{1}{M_1^2} + (1+\gamma)\varepsilon f_\xi\right] f_{\xi\xi} + 2\frac{kc}{U} f_{\xi\tau} - \frac{(\lambda c)^2}{M_1^2} f_{\eta\eta} - \left(\frac{c}{R}\right)^2 \frac{1}{M_1^2} f_{\zeta\zeta} = 0, \quad (4)$$

where $f(\xi,\eta,\zeta,\tau) = \phi'/c\varepsilon$ is the potential of small sound disturbances. Boundary condition (2) for the potential of small sound disturbances is written:

$$-f_\eta + \varepsilon f_\xi g_\xi = -g_\xi. \quad (5)$$

Thus, the calculated system of equations is (4), (5). The grid for the numerical calculation was chosen as follows: by coordinate ξ, the grid was chosen to be denser: $\xi_i, i = 1,...,80$. By the coordinate ζ, it was sparser: $\zeta_i, i = 1,...,40$. This computational grid made it possible to perform a stable numerical calculation

4. Near sound field

As mentioned above, the main interest of the study is to investigate the mutual influence of the blade geometry, its angles of insertion to the flow, and angles of attack on the nature of the generated noise. It is known today that noise generation of aerodynamic origin occurs as a result of small disturbances in the flow due to the interaction of the rotor blade and the flow. And the nonlinear term in Equation (1) plays an important role in the process of small disturbances generation [34]. This type of differential equations generate weak shock waves that transform into sound waves [35]. The near-field characteristic that determines the behaviour of small disturbances is the pressure coefficient $-C_p$.

The NASA parabolic cross-sectional profile of relative thickness δ=0.06 is used as a model in the calculations. The blade is placed in the flow at an angle of attack $\alpha=7^o,10^o$. The blade is twisted according to a linear law with a negative torsion equal to $\theta = 2^\circ$. The blade radius was R=23 cm, and the initial length of the blade cross-sectional chord was $c_{z=0}$=2.25 см and gradually decreased by the value $c_{z=R}$=2.15 см to the outer end of the blade. The calculation was carried out for three values of the rotor speed of the quadrotor Ω=2500;5000;7000 rpm, Mach number M = 0.1.

During the numerical calculations, the following values of the design parameters were chosen: the angle ψ of the blade to the flow was chosen $30^\circ, 60^\circ$, the negative torsion θ was decreasing at 2° to the end of the blade.

The results of numerical calculations for different blade angles to the flow, angles of attack, torsion and rotor speed showed the following. The pressure coefficient curves (Fig. 2, Fig. 3) show three separate series of peaks. The first series shows the unstable behaviour of small sound disturbances originating on the rotor blade surface during its streamlining. The irregular location of the local minimum and maximum indicates that the sound originates in the flow instability zone. This instability is caused by the interaction of the flow with the curved rotor blade of the quadrotor. It should be noted that a similar calculation carried out earlier for a helicopter blade without torsion [36] showed a more relaxed behaviour of pressure change $-C_p$. Thus, the presence of blade torsion generates instability in the flow, which is an additional factor in sound generation

As the flow continues to flow around the blade in cross-section, it begins to calm down. The second series of peaks is already clearly defined, without local sharp alternations of minimums and maximums. The level of the second series of peaks is twice that of the first series. This indicates that the sound generation in the second series is much greater than in the first series of peaks.

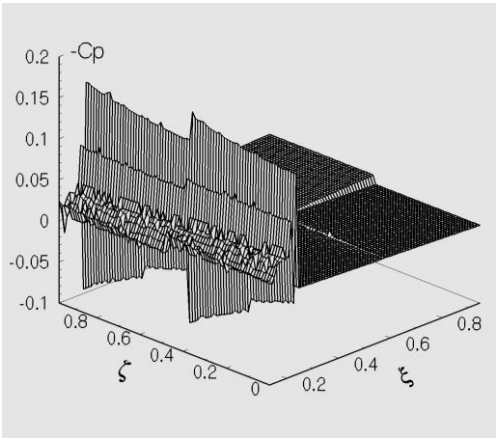

a) Ω=2500 prm, $\alpha=7^o$, $\psi = 30^\circ$

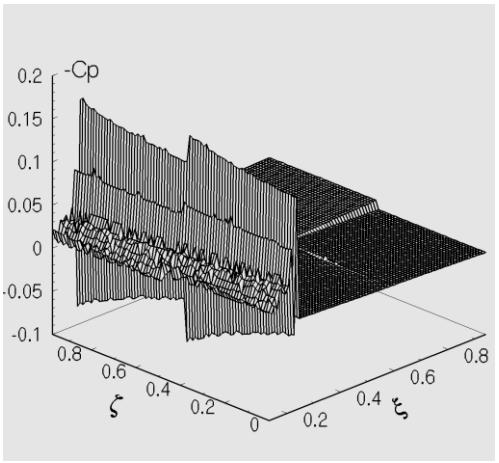

b) Ω=2500 prm, $\alpha=7^o$, $\psi=60^o$

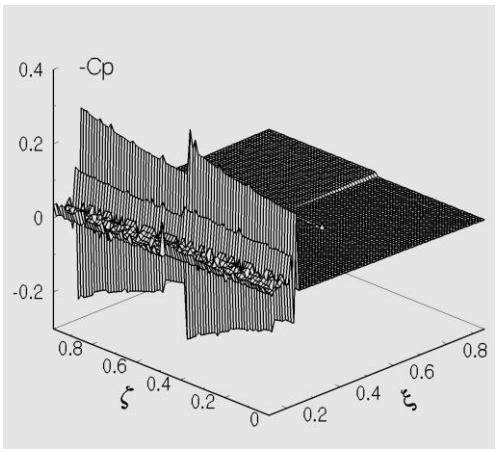

c) Ω=2500 prm, $\alpha=10^o$, $\psi=60^o$

Fig. 2 Pressure coefficient distribution on the blade surface

5. Far sound field

The obtained calculated data of the near-sound field of the quadrotor blade make it possible to use the integral representation to calculate the far-sound field [10]:

ISSN 1814-4225 (print)
АВІАЦІЙНО-КОСМІЧНА ТЕХНІКА І ТЕХНОЛОГІЯ, 2024, № 2(194) ISSN 2663-2012 (online)

$$4\pi\phi' = -M_1^2\int_S\left[\frac{1}{R}(\phi'_x+\frac{1}{2}(1+\gamma)(\phi'_x)^2\right]_{t^*}dS_x - \\ -\frac{2M_1^2}{U}\int_S\left[\frac{\phi'_t}{R}\right]_{t^*}dS_x + \\ +\int_S\left[\frac{1}{R}\frac{\partial\phi'}{\partial n}+\frac{1}{Ra_\infty}\frac{\partial R}{\partial n}\frac{\partial\phi'}{\partial t}-\phi'\frac{\partial}{\partial n}(\frac{1}{R})\right]_{t^*}dS. \quad (6)$$

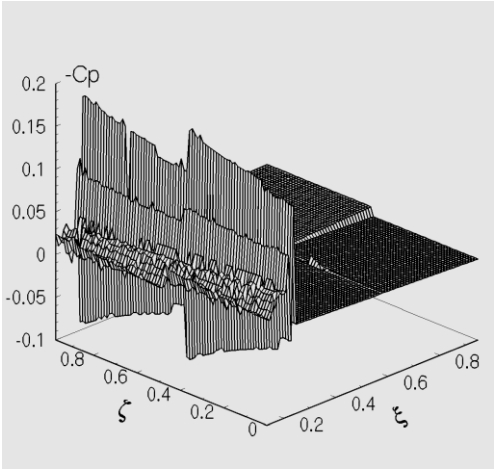

a) Ω=5000 prm , α=7° , ψ=30°

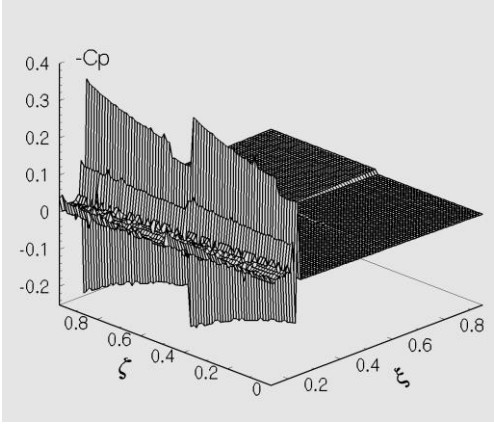

b) Ω=5000 prm , α=7° , ψ=60°

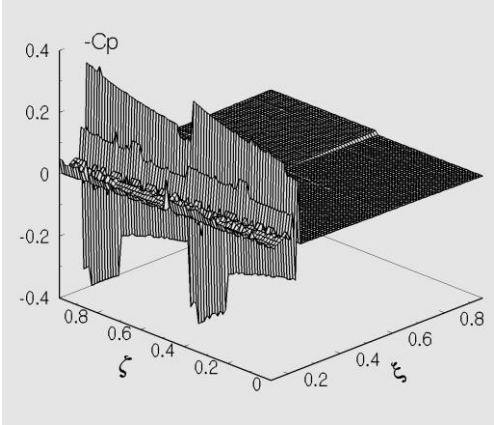

c) Ω=7000 prm , α=7° , ψ=60°

Fig. 3 Pressure coefficient distribution on the blade surface

An important characteristic of the distant sound field is the sound pressure level L. The numerical calculation of the sound pressure level at a distance y=0.1 m for different design cases is shown in Fig. 4, Fig. 5.

As can be seen from Fig. 4, Fig. 5, the maximum sound pressure level L for the same frequency for different angles of attack and blade angle varies within 3 dB: 95dB - 98dB. However, with an increase in rotational speed, Fig. 6, the sound pressure level increases significantly, approaching 110 dB.

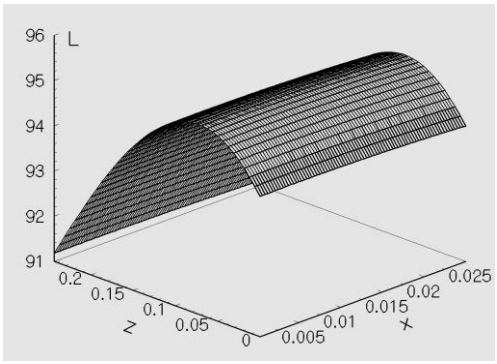

a) ψ=30°

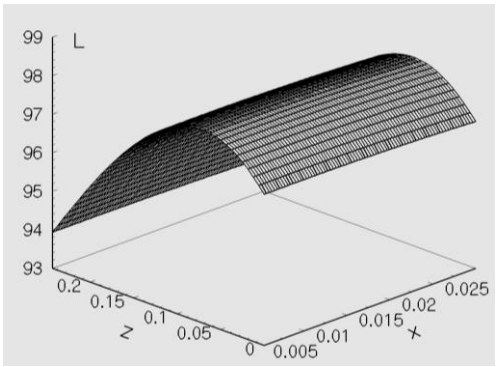

b) ψ=60°

Fig. 4. Sound pressure level, Ω=2500 prm , α=7°-5° angle of attack

It is known that the use of helicopter blade torsion allows for a more uniform force load on the blade. However, as mentioned above, blade torsion additionally disturbs the flow, which leads to additional sound generation. Nevertheless, the sound pressure level surfaces are smooth due to the torsion. The angle of attack of a helicopter rotor can be changed by means of a torsion device, thus adjusting the aerodynamic parameters of the helicopter. For quadcopters, the angle of attack of the blade does not change, so the aerodynamics of the blade and, consequently, the sound generation can be influenced only by the rotation frequency and the shape of the blade selected in advance. Thus, to solve the problem of reducing the noise of the quadrotor rotor, it is necessary to optimise the blade shape as a whole.

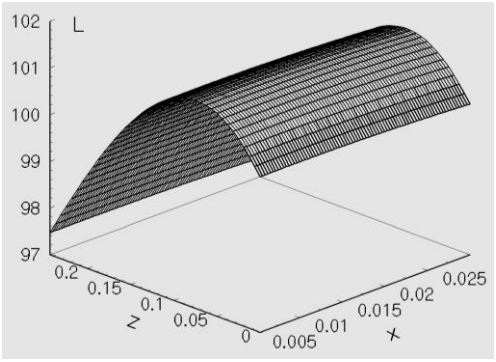

a) $\psi=30^o$

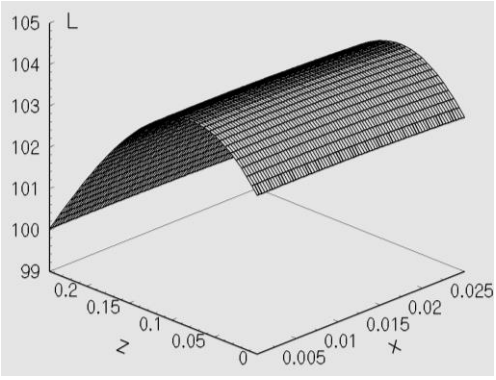

b) $\psi=60^o$

Fig. 5. Sound pressure level,
Ω=5000 prm , $\alpha=7^o$-5^o

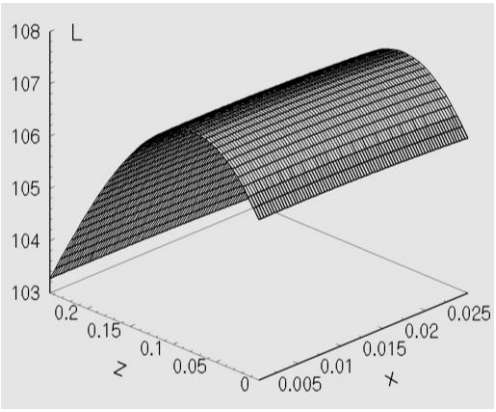

Fig. 6. Sound pressure level,
Ω=7000 prm , $\alpha=7^o$-5^o , $\psi=60^o$

The spectral analysis of the noise level showed (Fig. 7) that the frequency content of the noise is included in the first 6-7 harmonics, while the noise has a low- frequency predominance. Moreover, the maximum radiation is at the level of the first fundamental harmonic.

6. Calculation of blade noise in ANSYS

In order to compare the above numerical calculations of rotational noise, an additional calculation of aerodynamic noise was performed using ANSYS software. For the angle of attack $\alpha=5^o$ and flow velocity (M=0.475), rotation speed of 7000 rpm, a flow model around the profile was built. Fig. 8 shows the flow pattern around the profile, where the numbers 1, 2, 3, 4 indicate the reference points for sound registration.

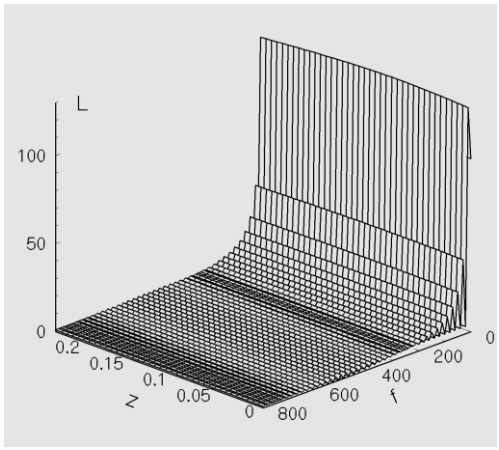

a) Ω=5000 prm

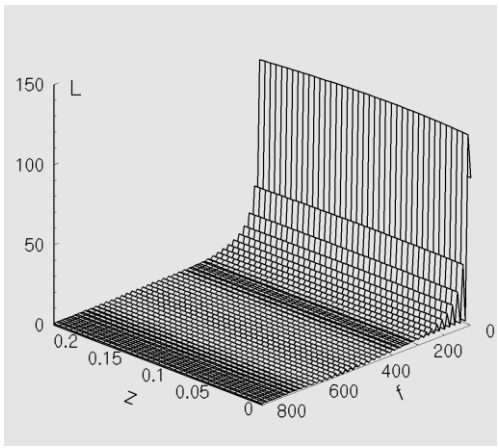

b) Ω=7000 prm

Fig. 7. Frequency spectrum, $\alpha=7^o$-5^o $\psi=30^o$

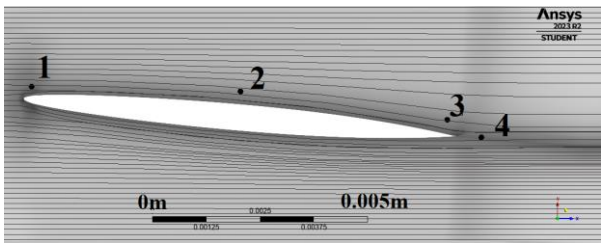

Fig. 8. Streamline of the profile and location of the sound study reference points for the 2d case

The centre of the coordinate system lies in the profile nose. Based on the results of the calculations, the graphs of the acoustic pressure dependence (Fig. 9) were constructed for different reference points in the flow. These dependences indicate the presence of unsteady sound pulsations in the flow. Using the Fourier transform with a Hamming filter, the spectra of sound vibrations (SPL) were constructed (Fig. 9). The

ISSN 1814-4225 (print)
ISSN 2663-2012 (online)

calculated time was t=0.01s. According to the Courant-Friedrichs-Levy criterion, the time step was respectively $\Delta t=5\times10^{-6}$s.

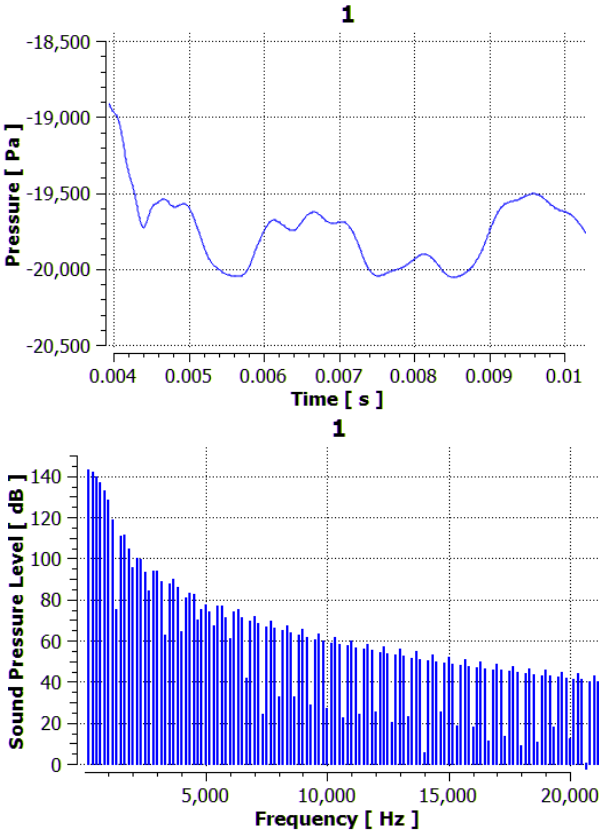

Fig. 9. Pressure and Sound Pressre Level at point 1

The graphs of sound pressure over time at reference points 1, 2, 3, 4 for the 2d case (see Fig. 8) obtained from the calculations are presented in Figs. 9-12. They show significant pulsations, which indicate the presence of a sound generation process, rotational noise, during the blade streamlining. Table 1 shows the coordinates of the sound recording points and the corresponding maximum pressure differences and maximum noise level in dB. The high value of the noise level, in the immediate vicinity of the blade is realised because in the representation of the far sound field (6), the distance to the blade R is in the denominator. And this representation has a similar form in all models without exception, including those implemented in ANSYS.

To obtain the sound characteristics at more distant areas from the blade, as well as for more realistic modelling, a 3D model of the screw was created (Fig. 13), as well as a model of its rotation in the ANSYS package. The sound characteristics were calculated at five reference points, Fig. 14. With an increase in the value of R, the noise level decreases significantly, and the sound wave turns into a homogeneous plane wave [10]. At the same time, the pressure change is uniform, Fig. 12

Table 1

Calculated data at points 1, 2, 3, 4 near the blade

Point No.	X, mm	Y, mm	Max Pressure Δ, Pa	Max SPL
1	0.20	0.33	1000	140
2	5.13	0.20	20	130
3	10.00	0.40	30	125
4	10.88	0.90	15	125

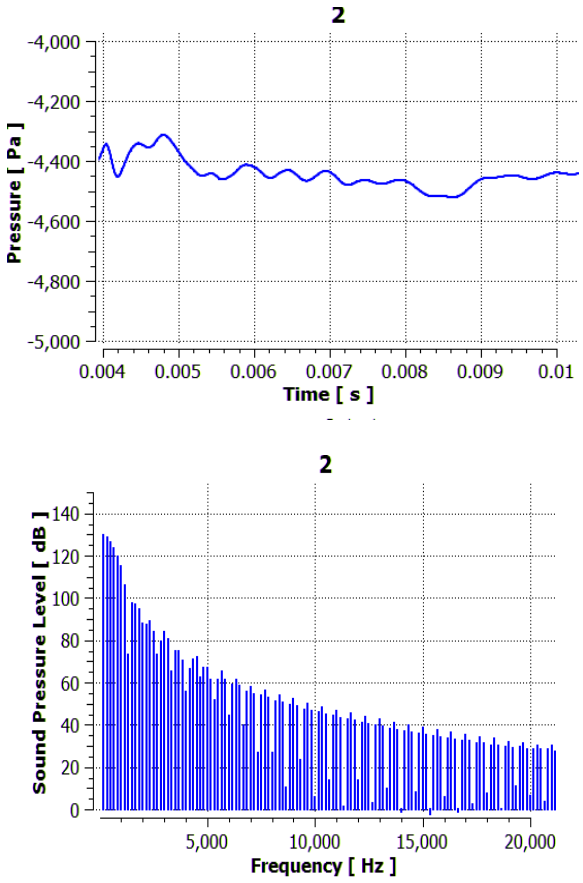

Fig. 10. Pressure and Sound Pressre Level at point 2

As we can see, the level in the noise spectrum at point 1, Fig. 13, reaches 80 dB at 233.3 Hz. Additional peaks in the spectrum are observed at frequencies of 466.6 Hz, 700 Hz, and 933.3 Hz. Thus, the rotation noise is dominated by the rotation frequency that has twice the propeller speed, i.e. the propeller speed multiplied by the number of blades. For all other points, however, these peaks are much less pronounced. In [26], the highest noise level was 78 dB, which closely coincides with the calculated data in Fig. 12. As noted in the comparison above, similar values of the sound pressure level, about 80 dB, are also given in [2, 14].

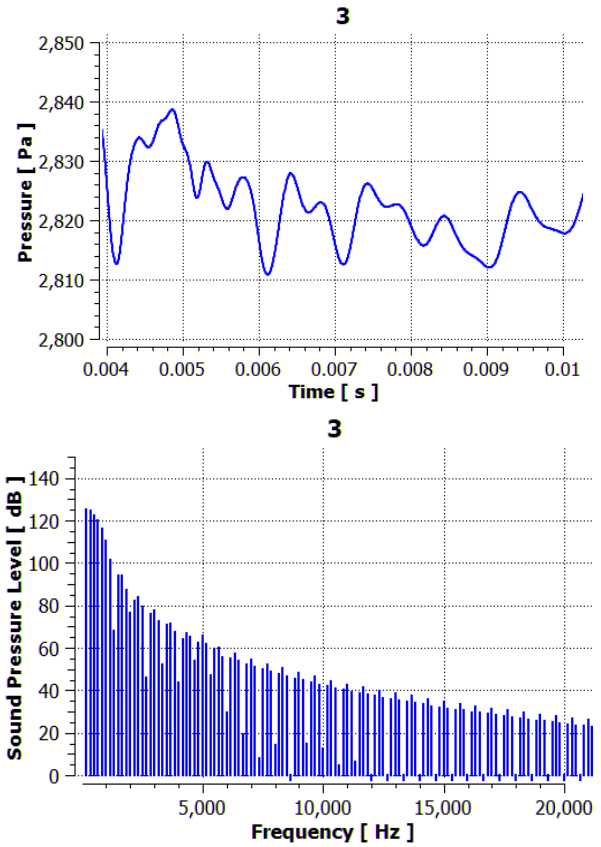

Fig. 11. Pressure and Sound Pressre Level at point 3

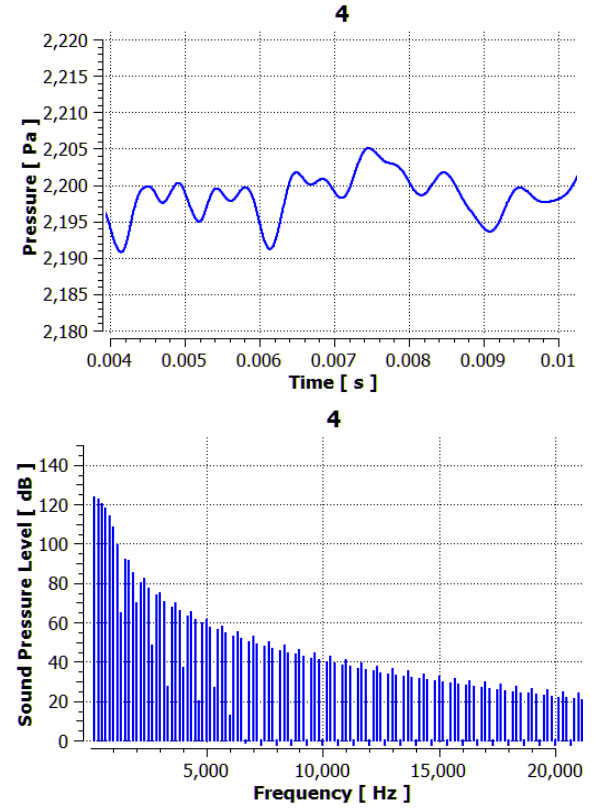

Fig.12 Pressure and Sound Pressre Level at point 4

Table 2 shows the distribution of the flow velocity on the blade v, Mach number M, chord length c, blade angle θ depending on the radial coordinate along the blade.

Table 2

Dependence of aerodynamic characteristics of the quadrocopter blade on the radial coordinate r

r cm	v m/s	M	c mm	θ
1	46.364	0.136	16.500	17.790
2	54.091	0.159	17.750	15.868
3	61.818	0,182	19.000	14.407
4	69.545	0.205	18.214	13.262
5	77.273	0.227	17.429	12.340
6	85.000	0.250	16.643	11.582
7	92.727	0.273	15.857	10.949
8	100.455	0.295	15.071	10.411
9	108.182	0.318	14.286	9.950
10	115.909	0.341	13.500	9.549
11	123.636	0.364	12.714	9.198
12	131.364	0.386	11.929	8.888
13	139.091	0.409	11.143	8.612
14	146.818	0.432	10.357	8.365
15	154.545	0.455	9.571	8.143
16	162.273	0.477	8.786	7.942
17	170.000	0.500	8.000	7.758

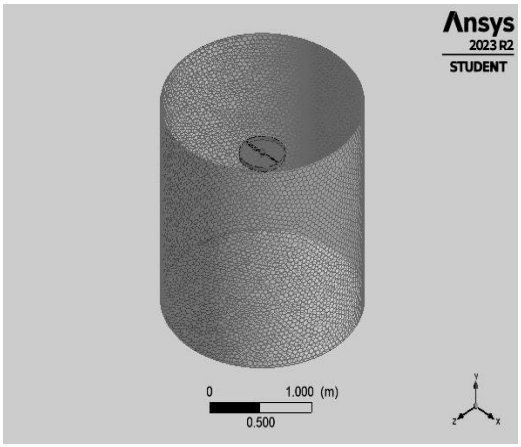

Fig. 13. Computational model of the propeller

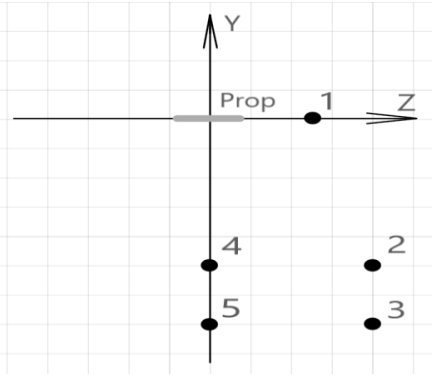

Fig. 14. Location of sound fixation points. The grid spacing is 0.2 m

ISSN 1814-4225 (print)
ISSN 2663-2012 (online)

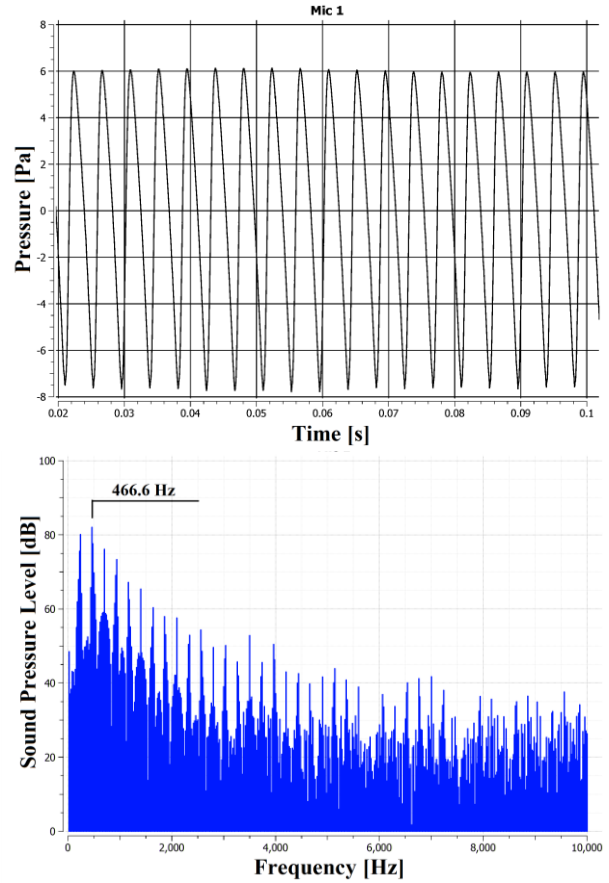

Fig. 15. Pressure value and noise spectrum at point 1 (0-10000 Hz)

As we can see, the noise spectrum level at the point 1 closest to the screw (Fig. 15) reaches 80 dB at 233.3 Hz. There are additional peaks in the spectrum at frequencies of 466.6 Hz, 700 Hz, and 933.3 Hz. Thus, the rotation noise is dominated by the rotation frequency that has twice the propeller speed, i.e. the propeller speed multiplied by the number of blades. For all other points, however, these peaks are much less pronounced. In [26], the highest noise level was 78 dB, which is close to the calculated data in Fig. 15. As noted in the comparison above, similar values of the sound pressure level, about 80 dB, are also given in [2, 14].

At points 2, 3, 4, 5, Figs. 16-19, 1 and 1.2 metres away from the propeller, the sound pressure level drops to 60 dB. These results confirm that this noise is mainly rotational noise.

We remind another interesting feature of this noise: in [24], it was found that doubling the distance to the propeller reduces the noise by 6 dB. This feature can be seen if we compare the spectra at reference points 2 and 4 (Figs. 15, 17) with the spectra at points 3 and 5 (Figs. 16, 18). Although this feature is less expressed, since the distance in this case was reduced not by a factor of 2 but by a factor of 1.4. It is also known [24] that rotational noise exceeds other types of noise by about 10 dB. Numerical calculations show a difference in sound pressure level from 20 dB to 40 dB. Such a significant discrepancy can be explained by the imperfection of modelling of noise sources of aerodynamic origin on the blade surface.

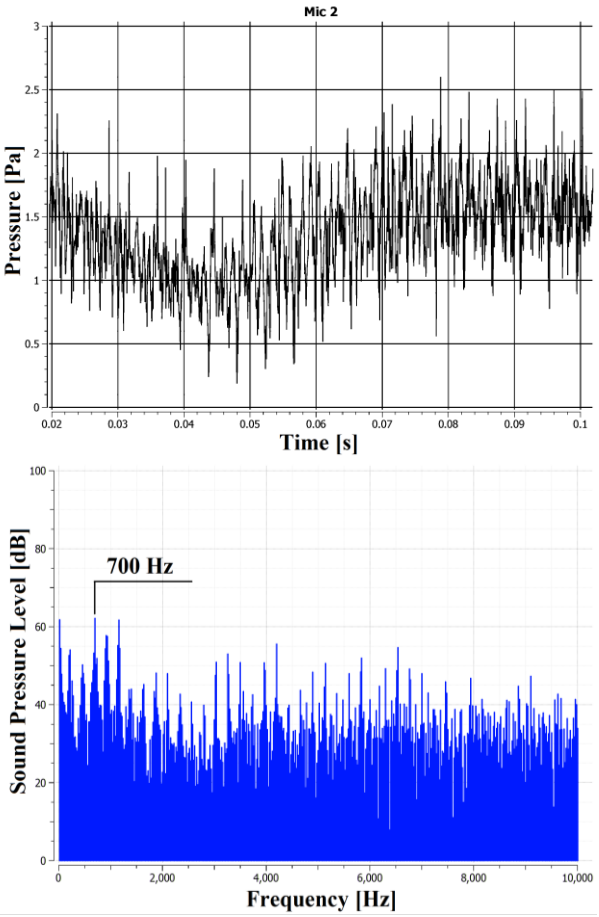

Fig. 16 Pressure value and noise spectrum at point 2 (0-10000 Hz)

It is worth to note that with distance from the propeller, the maximum sound pressure level at 233 Hz becomes less pronounced. In addition, with further distance from the blade, the sound source, the noise level at high frequencies decreases significantly, while at low frequencies it remains. This indicates that the far sound field has a predominantly low-frequency noise spectrum. The results obtained in ANSYS show that the main frequency content of the noise is contained in the first 6-7 harmonics and the energy of the sound, the rotational noise, is in the range of up to 2000 Hz.

Discussion

The results of the numerical studies performed by the potential model and using the ANSYS package showed an approximate coincidence of the calculated data. In particular, the noise level calculated using both models is within 80 dB. For the potential model, it is 76-78 dB, and for the model based on the FW-H

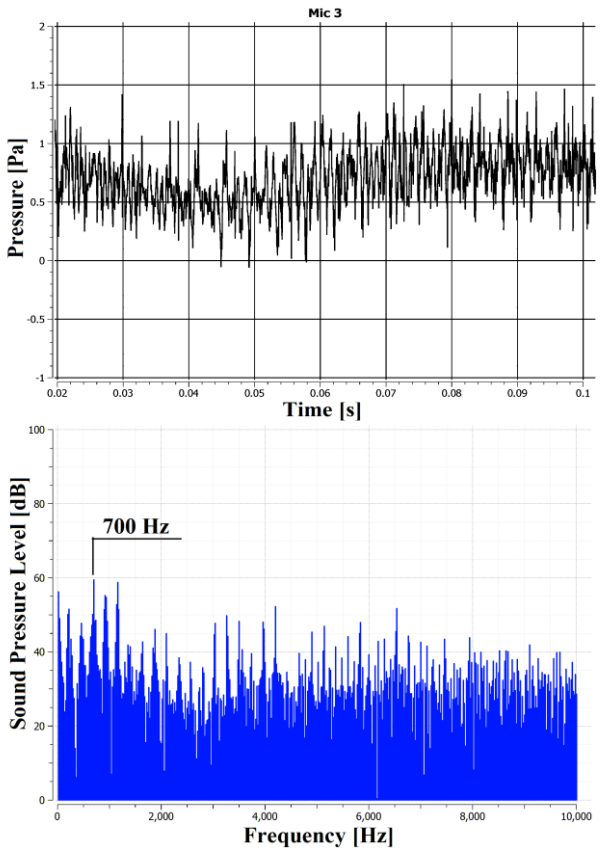

Fig. 17. Pressure value and noise spectrum at point 3 (0-10000 Hz)

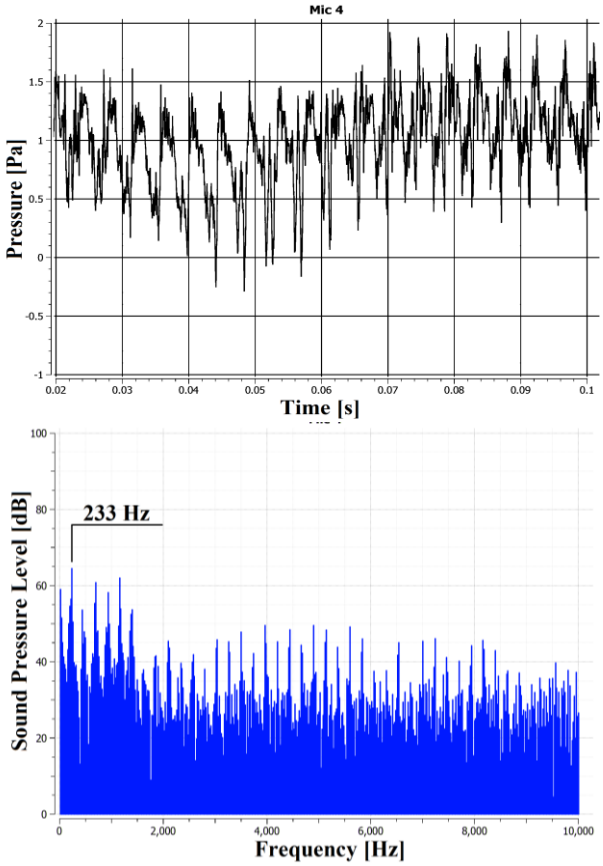

Fig. 18. Pressure value and noise spectrum at point 4 (0-10000 Hz)

equation, it is close to 80 dB. The values of the pressure level obtained in experimental studies are located between the values for the theoretical models just mentioned. Thus, there is a need, firstly, to improve and validate the new models, and also to find new more optimal blade shapes, since the noise generated by the blade is close to the noise limit of 85 dB.

Conclusions

The problem of generating rotational noise by a rotor blade of a small-sized quadrotor is formulated and numerically solved. A three-dimensional non-stationary model of generation and propagation of small disturbances from a thin wing - a quadrotor blade - is used.

The analysis of the obtained calculation data based on the numerical-analytical method has shown that a torsion blade generates a sound field by three series of disturbances located one after another along the blade cross-section. The first series of disturbances is unstable, which is the cause of the blade torsion. The next two series of peaks are smooth. The levels of the maximums in these series depend on the angle of the blade to the flow in the plane of rotation of the quadrotor rotor.

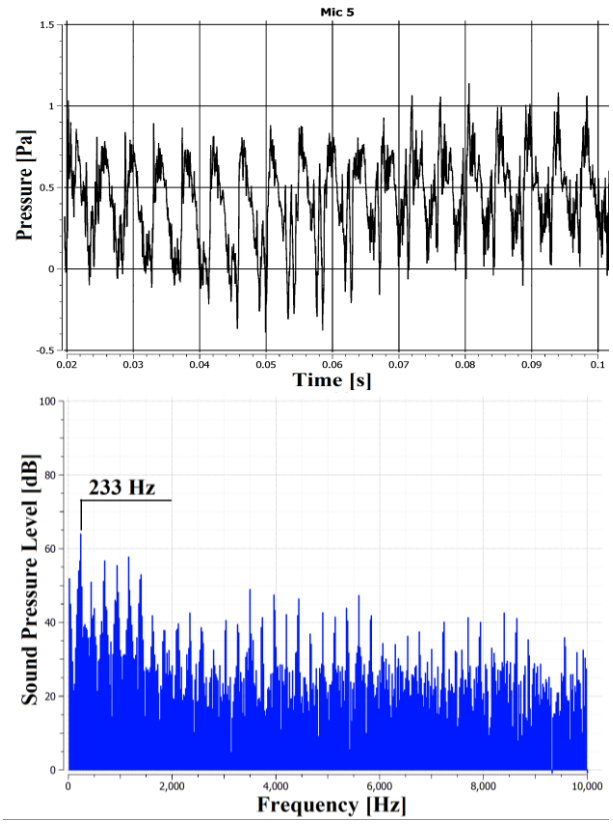

Fig. 19. Pressure value and noise spectrum at point 5 (0-10000 Hz)

ISSN 1814-4225 (print)
ISSN 2663-2012 (online)

The data of the far sound field calculation showed that in all calculated cases, without exception, the sound pressure level surface has a smooth character. The blade angle to the flow leads to a variation of the sound pressure level within 2 dB. At the same time, the dependence of the maximum sound pressure level on frequency is significant: from 95dB to 108dB. At a distance of 7-10 blade lengths, the numerical calculations showed the value of the maximum noise level to be in the range of 78dB-82dB, which coincides well with the calculated and experimental data of other authors. In addition, the calculations indicate that the main parameter that determines the noise level is the rotor speed, and the angle of attack in the far field does not affect the maximum noise level. The spectral content of the noise indicates the low-frequency nature of the rotation noise.

Aerodynamic calculations and noise generation around the quadcopter blade using ANSYS software revealed that sound vibrations of up to 120 dB occur when the blade tip flows around the blade. Calculations using a 3d model of the propeller confirmed that the sound pressure level was already 80 dB at the nearest reference point. At a distance of about 5-6 blade lengths, the noise level drops to 60 dB, which is consistent with the results of other studies, as well as the studies in paragraphs 1-5 of this paper.

The obtained results of numerical calculations will be used in the future to find the optimal low-noise shape of the quadrotor blade.

Contribution of authors: Setting problem, numerical calculation with use of potential approach – **Petro Lukianov**, **Oleg Dusheba**; calculation the problem with use of ANSYS software software – **Oleg Dusheba**; development of mathematical model – **Petro Lukianov**; analysis of results – **Petro Lukianov**, **Oleg Dusheba**.

Conflict of Interest

The authors declare that they have no conflict of interest in relation to this research, whether financial, personal, authorship or otherwise, that could affect the research and its results presented in this paper.

Financing

The research was conducted without financial support.

Data availability

The work has no associated data.

Use of Artificial Intelligence

The authors confirm that they did not use artificial intelligence methods while creating the presented work.

All the authors have read and agreed to the published version of this manuscript.

References

1. Environmental Protection Technical Specifications applicable to VTOL-capable aircraft powered by non-tilting rotors. *EASA*, 2023, iss. 1. 71 p. Available at: https://www.easa.europa.eu/en/downloads/139022/en. (accessed 12.01.2024).

2. Kevin Li, S. An Analytic Method to Predict Rotor Blade Wake Interaction. *VFS' 79th Annual Forum & Technology Display*, May 16-18, 2023 Palm Beach County Convention Center, West Palm Beach, Florida, pp. 1-12. DOI: 10.4050/F-0079-2023-17953.

3. Kevin Li, S., & Lee, S. Acoustic Analysis and Sound Quality Assessment of a Quiet Helicopter for Air Taxi Operations. *Journal of the American Helicopter Society*, 2022, vol. 67, iss. 3, pp. 1-15. DOI: 10.4050/JAHS.67.032001.

4. Froude, W. On the Elementary Relation between Pitch, Slip and Propulsive Efficiency. *Transaction of the Institute of Naval Architects*, 1878, vol. 19, pp. 22-33.

5. Farassat, F., & Myers, M. K. Extension of Kirchhoff's Formula to Radiation from Moving Surfaces. *Journal of Sound and Vibration*, 1988, vol. 123, iss. 3, p. 451-461. DOI: 10.1016/S0022-460X(88)80162-7.

6. Romani, G., Grande, E., Avallone, F., Ragni, D., & Casalino, D. Perforence and noise prediction of low-Reynolds number propellers using the Lattice-Boltzmann method. *Aerospace Science and Technology*, 2022, vol. 125, article no. 107086. DOI: 10.1016/j.ast.2021.107086.

7. Jonson, W., & Silva, C. NASA concept vehicles and the advanced air mobility aircraft. *The Aeronautical Journal*, 2022, vol. 126, special iss. 1295, pp. 59-91. DOI: 10.1017/aer.2021.92.

8. Kostek, A. A., Lößle, F., Wickershein, R., Keßler, M., Boisaerd, R., Reboul, G., Visingardi, A., Bartarino, M., & Gardner, A. D. Experimental investigation of UAV rotor aeroacoustics and aerodynamics with computational cross-validation. *CEAS Aeronautical Journal*, September 2023. DOI: 10.1007/s13272-023-00680-z.

9. Yin, J., Rossignol, K.-S., Rottmann, L., & Schwarz, T. Numerical studies on small rotor confgurations with validation using acoustic wind tunnel data. *CEAS Aeronautical Journal*, June 2023. DOI: 10.1007/s13272-023-00671-0.

10. Lukianov, P. V. Nestatsionarnoye rasprostraneniye malykh vozmushcheniy ot tonkogo kryla: blizhneye i dal'neye pole [Nonstationary propagation of small disturbances from a thin wing: near and far field]. *Akustychnyi visnyk – Acoustic Herald*, 2009, vol.12, iss. 3, pp. 41-55. Available at: https://hydromech.org.ua/content/uk/av/av-12-3.html. (accessed 11.02.2024).

11. Škultéty, F., Bujna, E., Janovec, M., & Kandera, B. Noise Impact Assessment of UAS Operation in Urbanised Areas: Field Measurements and a Simulation.

Drones, 2023, vol. 7, iss. 5, article no. 314. DOI: 10.3390/drones7050314.

12. *Unmanned Aircraft Systems Consolidated version of Regulation (EU) 2019/947 as retained (and amended in UK domestic law) under the European Union (Withdrawal), Act 2018 CAP1789A*. Available at: https://www.caa.co.uk/publication/download/17981 (accessed 12.11.2023).

13. Thurman, C. S., & Baeder, J. D. Blade-Wake Interaction Noise for Hovering sUAS Rotors, Part I: Characterization Study. *AIAA Journal*, 2023, vol. 61, no. 6. DOI: 10.2514/1.J062565.

14. Sinibaldi, G., & Marino, L. Experimental analysis on the noise of propellers for small UAV. *Applied Acoustics*. 2013, vol. 74, iss. 1, pp. 79-88. DOI: 10.1016/j.apacoust.2012.06.011.

15. Gur, O., & Rosen, A. Design of a Quiet Propeller for an Electric Mini Unmanned Air Vehicle. *Journal of Propulsion and Power*, 2009, vol. 25, iss. 3, pp.717-728. DOI: 10.2514/1.38814.

16. Cussen, K., Garruccio, S., & Kennedy, J. UAV Noise Emission—A Combined Experimental and Numerical Assessment. *Acoustics*, 2022, vol. 4, iss. 2, pp. 297-312. DOI: 10.3390/acoustics4020018.

17. Roger, M., & Moreau, S. Tonal-noise assessment of quadrotor-type UAV using source-mode expansions. *Acoustics*, 2020, vol. 2, iss. 3, pp. 674-690. DOI: 10.3390/acoustics2030036.

18. Gutin, L. On the Sound Field of a Rotating Propeller. *NACA Technical Memorandum No. 1195*, Washigton, 1948. 22 p. Available at: https://ntrs.nasa.gov/api/citations/20030068996/downloads/20030068996.pdf (accessed 12.1.2024).

19. Kim, D. H., Park, C. H., & Moon, Y. J. Aerodynamic analyses on the steady and unsteady loading-noise sources of drone propellers. *Int. J. Aeronaut. Space Sci.*, 2019, vol. 20, pp. 611-619. DOI: 10.1007/s42405-019-00176-3.

20. Han, D., Gwak, D. Y., & Lee, S. Noise prediction of multi-rotor UAV by RPM fluctuation correction method. *Journal of Mechanical Science and Technology*, 2020, vol. 34, iss. 4, pp. 1429-1443. DOI: 10.1007/s12206-020-0305-2.

21. Noda, R., Ikeda, T., Nakata, T., & Liu, H. Characterization of the low-noise drone propeller with serrated Gurney flap. *Frontiers in Aerospace Engineering*, 2022, vol. 1, pp. 1-13. DOI: 10.3389/fpace.2022.1004828.

22. Intaratep, N., Alexander, W. N., Devenport, W. J., Grace, S., & Dropkin, M. A. Experimental Study of Quadcopter Acoustics and Performance at Static Thrust Conditions. *22nd AIAA/CEAS Aeroacoustics Conference*, 2016, 30 May - 1 June, Lyon, France. Available at: https://www.bu.edu/ufmal/files/2016/07/aiaa-2016-2873.pdf. (accessed 12.01.2024).

23. Kelecy, Fr. J. An Examination of Quadcopter Drone Noise Using Computational Aeroacoustics. *ANSYS Inc. Advanced Modeling & Simulation (AMS) Seminar Series NASA Ames Research Center*, October 14, 2021. 47 p. Available at: https://www.nas.nasa.gov/assets/nas/pdf/ams/2021/AMS_20211014_Kelecy.pdf. (accessed 12.11.2023).

24. Massey, K., & Gaeta, R. Noise Measurements of Tactical UAVs. *16th AIAA/CEAS Aeroacoustics Conference*. DOI: 10.2514/6.2010-3911.

25. Kloet, N., Watkins, S., & Clothier, R. Acoustic signature measurement of small multi-rotor unmanned aircraft systems. *International Journal of Micro Air Vehicles*, 2017, vol. 9, iss. 1, pp. 1-14. DOI: 10.1177/1756829316681868.

26. Heydari, M., Sadat, H., & Singh, R. A Computational Study on the Aeroacoustics of a Multi-Rotor Unmanned Aerial System. *Appl. Sci.*, 2021, vol. 11, iss.20, article no. 9732. DOI: 10.3390/app11209732.

27. Lukianov, P. V. Vplyv formy, kryvyzny poperechnoho pererizu lopati rotora na parametry shumu obertannya [The influence of the shape and curvature of the cross section of the rotor blade on the parameters of rotation noise]. *Naukovi visti NTUU «KPI» : mizhnarodnyy naukovo-tekhnichnyy zhurnal – Scientific news of NTUU "KPI": international scientific and technical journal*, 2012, vol. 4(84), pp. 149-153. Available at: https://ela.kpi.ua/items/27584f07-8247-41ad-bbe0-d3300128ee95. (accessed 2.02.2024).

28. Lukianov, P., & Dusheba, O. Modeling of Aerodynamic Noise of Quadrotor Type Aerotaxis. *Aviacijno-kosmicna tehnika i tehnologia – Aerospace technic and technology*, 2023, vol. 4, pp. 38-49. DOI: 10.32620/aktt.2023.4.05.

29. Caradonna, F. X., & Isom, M. P. Subsonic and Transonic Potential Flow over Helicopter Rotor Blades. *AIAA Journal*, 1972, vol. 10, iss.12, pp. 1606-1612. DOI: 10.2514/3.50404.

30. Caradonna, F., X., & Isom, M., P. Numerical Calculation of Unsteady Transonic Potential Flow over Helicopter Rotor Blades. *AIAA Journal*, 1976, vol. 14, iss.4, pp. 482-488. DOI: 10.2514/3.61387.

31. Ballhaus, W. R., & Goorjian, P. M. Implicit finite-Difference Computations of Unsteady Transonic Flows about Airfoils. *AIAA Journal*, 1977, vol. 15, iss. 12, pp. 1728-1735. DOI: 10.2514/3.60838.

32. Lukianov, P. V. Ob odnom chislenno-analiticheskom podkhode k resheniyu zadachi generatsii zvuka tonkim krylom. Chast' I. Obshchaya skhema primeneniya dlya ploskoy statsionarnoy zadachi [About one numerical-analytical approach to solving the problem of sound generation by a thin wing. Part I. General scheme of application for a plane stationary problem]. *Akustychnyi visnyk – Acoustic Herald*, 2011, vol. 14, iss. 3, pp. 46-52. Available at: http://hydromech.org.ua/content/uk/av/av-14-3.html. (accessed 11.02.2024).

33. Lukianov, P. V. Ob odnom chislenno-analiticheskom podkhode k resheniyu zadachi generatsii zvuka tonkim krylom. Chast' II. Skhema primeneniya dlya nestatsionarnykh zadach [About one numerical-analytical approach to solving the problem of sound generation by a thin wing. Part II. Application diagram for non-stationary tasks]. *Akustychnyi visnyk – Acoustic Herald*, 2012, vol.15, iss. 3, pp. 45-52. Available at:

http://hydromech.org.ua/content/ru/av/15-3_45-52.html. (accessed 11.02.2024).

34. Von Karman, T. The similarity low of transonic flow. *Journal of Math. and Phisics*, 1947, vol. 26, iss. 1-4, pp. 182-190. DOI: 10.1002/SAPM1947261182.

35. Courant, R., & Friedrichts, K. O. *Supersonic Flow and Shock Waves*, Interscience Publishers, 1948. 440 p. Available at: https://books.google.mw/books?id=Qsxec0QfYw8C&printsec=frontcover&source=gbs_vpt_read#v=onepage&q&f=false. (accessed 11.02.2024).

36. Lukianov, P. V. Vplyv formy, kryvyzny poperechnoho pererizu lopati rotora helikoptera na parametry shumu obertannya [The influence of the shape and curvature of the cross-section of the helicopter rotor blade on the parameters of rotation noise]. *Naukovi visti NTUU «KPI» : mizhnarodnyy naukovo-tekhnichnyy zhurnal – Scientific news of NTUU "KPI": international scientific and technical journal*, 2012, no. 4, pp. 149-153. Available at: https://ela.kpi.ua/bitstream/123456789/36878/1/2012-4-25.pdf. (accessed 11.02.2024).

Надійшла до редакції 15.01.2024, прийнята до опублікування 15.04.2024

ЧИСЕЛЬНЕ ДОСЛІДЖЕННЯ ВПЛИВУ ПАРАМЕТРІВ ЛОПАТІ КВАДРОКОПТЕРА НА ГЕНЕРАЦІЮ ШУМУ АЕРОДИНАМІЧНОГО ПОХОДЖЕННЯ

П. В. Лук'янов, О. В. Душеба

Предметом даної роботи є дослідження впливу варіації параметрів лопаті малих розмірів квадрокоптера на рівень шуму аеродинамічного походження, його частотний спектр. Наявні сьогодні розрахункові та експериментальні дані мають певну розбіжність. Причина полягає у тому, що вивчення шуму ротора квадрокоптера відбувається із застосуванням різних теоретичних моделей, що не враховують окремих чинників виникнення звуку або враховують додаткові штучні джерела звуку, що в результаті дають завищений рівень шуму. Отже виникла необхідність у точній моделі, розрахунок шуму з використанням якої більш точно відповідає експериментальним даним. У нижче наведеній роботі запропоновано модель шуму аеродинамічного походження для вивчення шуму лопаті квадрокопетра, що враховує нестаціонарність та тривимірність процесу генерації та поширення звуку. **Методи дослідження засновані на** чисельному розрахунку характеристик ближнього та дальнього звукових полів у потенціальному наближенні: коефіцієнту тиску, рівня звукового тиску, спектру генерованого звука. Основними параметрами, що варіювались в процесі чисельних розрахунків, були частота обертання ротора квадрокоптера, кута атаки, кут крутки та постановки лопаті у площині обертання. У якості тестового профілю розглінуто параболічний профіль NASA. **Результати та висновки**. Результати числових розрахунків у ближньому полі виявили три області генерації звуку над поверхнею лопаті. Причому перша область, більш нестійка, спричинена круткою лопаті. Решта дві області генерації звуку є плавно розподіленими уздовж розмаху лопаті і рівень зміни тиску у кожній з них подвоюється. Рівень генерованого шуму аеродинамічного походження значною мірою залежить від частоти обертання лопаті та відстані від лопаті, на якій цей шум розраховується. Кут атаки та кут постановки лопаті менше впливає на рівень генерованого шуму, а в дальньому поля – майже не впливає на максимальний рівень шуму. Залежність шуму від відстані до лопаті, а також параметри лопаті, що обирались подібними таким, які досліджували інші автори, показали достатньо хорошу збіжність з розрахунками даних авторів, а також з експериментальними дослідженнями. У результаті аеродинамічних розрахунків та генерації шуму навколо лопаті квадрокоптера з використанням програмного забезпечення ANSYS, було встановлено, що під час обтіканні кінцевої частини лопаті виникають звукові коливання, рівень яких сягає 120 дБ у безпосередній близкості до поверхні лопаті. Розрахунки з використанням 3D моделі гвинта підтвердили, що гучність сягає 80 дБ у найближчій реперній точці, що наближено співпадає з даним розрахунку на основі потенціальної моделі, а також з даними ескперимента.

Ключові слова: шум аеродинамічного походження; числові методи; квадрокоптер.

Лук'янов Петро Володимирович – канд. фіз.-мат. наук, старш. наук. співроб., доц. каф. авіа- та ракетобудування, Національний технічний університет України «КПІ ім.Ігоря Сікорського», Київ, Україна.

Душеба Олег Володимирович – магістр, асп. каф. авіа- та ракетобудування, Національний технічний університет України "КПІ ім.Ігоря Сікорського", Київ, Україна.

Petro Lukianov – Candidate of Physics and Mathematics Sciences, Senior Researcher, Associate Professor of the Department of Avia- and rocket constructions, National Technical University of Ukraine "KPI named after Igor Sikorsky", Kyiv, Ukraine,
e-mail: p.lukianov@kpi.ua, ORCID: 0000-0002-7584-1491.

Oleg Dusheba – Master of Technical Sciences, PhD student of the Department Avia- and rocket constructions, National Technical University of Ukraine "KPI named after Igor Sikorsky", Kyiv, Ukraine,
e-mail: olegdusheba@gmail.com, ORCID: 0000-0002-0033-2414.